Heliyon 10 (2024) e33738

Contents lists available at ScienceDirect

Heliyon

journal homepage: www.cell.com/heliyon

Research article

Identification of lncRNA-mRNA network linking ferroptosis and immune infiltration to colon adenocarcinoma suppression

Xiao-Qiong Chen [a,*,1], Xuan Zhang [a,1], Ding-Guo Pan [a,1], Guo-Yu Li [a], Rui-Xi Hu [a], Tao Wu [a], Tao Shen [a], Xin-Yi Cai [a], Xian-Shuo Cheng [a], Junying Qin [c], Fu-Hui Xiao [b,***], Yun-Feng Li [a,**]

[a] *Colorectal Surgery, Third Affiliated Hospital of Kunming Medical University, Yunnan Cancer Hospital, Peking University Cancer Hospital Yunnan, Kunming, 650000, China*

[b] *State Key Laboratory of Genetic Resources and Evolution, Kunming Institute of Zoology, Chinese Academy of Sciences, Kunming, 650000, China*

[c] *CAS Key Laboratory of Genomics and Precision Medicine, Beijing Institute of Genomics, Chinese Academy of Sciences, China National Center for Bioinformation, Beijing, 100101, China*

ARTICLE INFO

Keywords:
Colon adenocarcinoma
Ferroptosis
Tumor immune microenvironment
Transcriptome
Neutrophil

ABSTRACT

Background: Colon adenocarcinoma (COAD) is one of the most common malignant tumors. The interplay involving ferroptosis between tumor and immune cells plays a crucial in cancer progression. However, the biological basis of this interplay in COAD development remains elusive.
Methods: Transcriptome data of COAD samples were obtained from The Cancer Genome Atlas and National Center for Biotechnology Information databases. Using single-sample gene set enrichment analysis, we calculated the ferroptosis score (FS) and immune cell infiltration levels for each sample, leveraging the expression levels of genes related to ferroptosis and various immune cell types. Samples with FSs greater than the 75th percentile were classified into the high-FS subgroup, while those below the 25th percentile were categorized as the low-FS subgroup. Moreover, tumor tissue samples and adjacent normal tissue samples were collected from twenty colon patients. Using real-time quantitative polymerase chain reaction, we validated the expression of certain genes in these samples.
Results: The COAD samples with high FSs experienced favorable survival probability and heightened sensitivity to anticancer drugs, with FSs negatively associated with the pathological stages. Moreover, the up-regulated genes in high-FS subgroup exhibited enrichment in immune-related pathways, suggesting a correlation between immunity and ferroptosis. Importantly, we discovered a key lncRNA-mRNA co-expression network linking tumor cell ferroptosis and immune infiltration (e.g., neutrophil) in the progression and classification of COAD. Further analysis identified several ferroptosis-related lncRNAs (e.g., *RP11-399O19.9*) within this network, indicating their potential roles in COAD progression and deserving in-depth study.

* Corresponding author. Third Affiliated Hospital of Kunming Medical University, Tumor Hospital of Yunnan Province, Kunming, 650000, China.
** Corresponding author. Third Affiliated Hospital of Kunming Medical University, Tumor Hospital of Yunnan Province, Kunming, 650000, China.
*** Corresponding author.
E-mail addresses: chenxiaoduoycc@126.com (X.-Q. Chen), agingstudy_xiao@163.com, xiaofuhui@mail.kiz.ac.cn (F.-H. Xiao), liyunfeng001@foxmail.com, liyunfeng@medmail.com.cn (Y.-F. Li).
[1] These authors contributed equally to this work.

https://doi.org/10.1016/j.heliyon.2024.e33738
Received 7 April 2024; Received in revised form 1 June 2024; Accepted 26 June 2024
Available online 27 June 2024
2405-8440/© 2024 The Authors. Published by Elsevier Ltd. This is an open access article under the CC BY-NC license (http://creativecommons.org/licenses/by-nc/4.0/).

Conclusions: Our findings provide novel insights into the underlying biological basis, particularly involving lncRNAs, at gene expression level associated with ferroptosis in COAD and cancer therapy. Nevertheless, further analysis and validation are required to expand the findings.

1. Introduction

Colon adenocarcinoma (COAD) is the third most common cancer and second most frequent cause of cancer death worldwide [1]. Despite advancements in clinical diagnosis and treatment for COAD, both its incidence and mortality rates persistently rise [2,3]. The pronounced heterogeneity of COAD, evident across various molecular levels, poses a significant challenge in disease diagnosis and therapy [4,5]. Therefore, there remains an urgent need for research on the underlying molecular mechanism involved to the classification and progression of COAD.

Ferroptosis is an iron-dependent and distinct form of regulated cell death. It differs from other forms of regulated cell death (e.g., necroptosis, apoptosis, and autophagy) and is associated with pathological processes in various tumors, such as breast cancer, hepatocellular carcinoma, ovarian cancer, and COAD [6–10]. Additionally, a growing body of literature highlights the involvement of ferroptosis in the crosstalk between tumor cells and immune cells within tumor microenvironment [11–14]. Cancer cells undergoing ferroptosis can release immune-regulatory factors, influencing the functions of neighboring immune cells, which, in turn, also regulate the ferroptosis activity of cancer cells. For instance, one study demonstrates that activated $CD8^+$ T cells induce ferroptosis in tumor cells through the secreted interferon-γ (IFN-γ) [11], while another reveals that early ferroptotic cancer cells exhibit specific immunogenicity and enhance subsequent antitumor immune responses [12]. Therefore, gaining a better understanding of the biological basis underlying both tumor cell ferroptosis and the tumor immune microenvironment (TIME) could offer novel insights into the progression and therapy of COAD.

Long non-coding RNAs (lncRNAs) are RNA molecules with >200 nucleotides in length that do not encode functional proteins [15]. They have the capability to modulate gene expression at various levels, including interactions with DNA, RNA, and proteins [15]. The dysregulation of lncRNA is well-recognized for its significant role in tumor progression. Furthermore, emerging evidence supports strong associations between lncRNAs and both tumor ferroptosis and TIME, achieved through the regulation of target gene expression [16–18]. Despite these advances, the lncRNA-mRNA co-expression networks associated to ferroptosis and TIME relevant to COAD progression and classification have not yet been fully explored.

The objective of this study is to explore the transcriptional characteristics of lncRNA and mRNA that underlie the association between ferroptosis and TIME in COAD. This involves employing various analytical methods such as single-sample gene set enrichment analysis, survival analysis, differential expression analysis, weighted correlation network analysis, and functional enrichment analysis for COAD's transcriptome data. This scientific significance of this study lies in identifying the lncRNA-mRNA co-expression networks, as well as key genes, that potentially elucidate the regulatory mechanisms linking ferroptosis and TIME in COAD progression.

2. Materials and Methods

2.1. Data collection and preprocessing

Transcriptome (RNA-seq, HTSeq-Counts/log2(FPKM (fragments per kilobase of transcript per million fragments mapped) +1)) and clinical data of COAD samples included 446 COAD tumor samples and 39 adjacent normal samples, were obtained from The Cancer Genome Atlas (TCGA) database using the UCSC Xena platform (https://xena.ucsc.edu/) [19]. The expression levels of mRNAs and lncRNAs were transformed into FPKM values. In addition, an independent gene expression matrix of COAD was download from the National Center for Biotechnology Information (NCBI) GEO (Gene Expression Omnibus) DataSets with accession number GSE39582, which included 566 tumor samples and 19 adjacent normal samples [20]. After removing genes with missing values, 20,579 genes were analyzed in the TCGA dataset, 15,230 genes were analyzed in the NCBI dataset. For each dataset, the matrix was normalized using the 'normalize.quantiles' function in the R "preprocessCore" (v1.64.0) package (https://bioconductor.org/), as reviewed in Bolstad's study [21].

2.2. Inference of ferroptosis score (FS)

A total of 385 ferroptosis-related mRNA genes (ferr-mRNAs), including drivers, suppressors, and markers, were obtained from the FerrDb (V2) database [22]. Subsequently, we conducted Pearson's correlation test to identify the lncRNAs that significantly co-expressed with these genes based on the transcriptome data from the TCGA database, applying a threshold of P-value <0.00001 and an absolute value of correlation coefficient >0.4. To further screen the lncRNAs associated not only with ferroptosis but also COAD survival, we performed univariate Cox survival analysis to select 89 ferroptosis-related lncRNA genes (ferr-lncRNAs), with their expression positively (30) or negatively (59) associated with COAD overall survival (P-value <0.05). To infer a FS characterizing the ferroptosis level and survival potential in each sample, we respectively estimated the enrichment scores of lncRNA gene sets positively or negatively associated with COAD survival in each sample using single sample gene set enrichment analysis (ssGSEA) in the R package "GSVA" (v1.50.0) (https://bioconductor.org/) [23]. We defined the difference in enrichment scores between positive and negative components as the FS for each sample. Samples with FSs larger than the 75th percentile FS value were classified into high-FS

subgroup, while those with FSs smaller than 25th percentile FS value were classified into low-FS subgroup. Furthermore, we also estimated the FS of each sample retrieved from the NCBI database based on the expression levels of aforementioned ferr-lncRNAs.

2.3. Drug response sensitivity analysis in COAD samples

We downloaded the cancer cell line drug sensitivity data (half-maximal inhibitory concentration (IC50); low IC50 value represents high drug sensitivity) from the Genomics of Drug Sensitivity in Cancer database (GDSC, https://www.cancerrxgene.org/) [24,25]. The drug sensitivity score of each COAD samples obtained from the TCGA and NCBI databases was estimated based on gene expression data using the R package "oncoPredict" (v0.2) (https://cran.r-project.org/) [26]. Drugs with a mean predicted sensitivity value > 0.5 in the samples were removed. Differences in response sensitivity to each drug between the two COAD subgroups were tested using Student's *t*-test. $P < 0.05$ was considered statistically significant.

2.4. Survival analysis

Kaplan-Meier plots and log-rank tests were used to evaluate survival differences between two subgroups within either the TCGA or NCBI database, respectively, using the R package "survival" (v3.5-7) (https://cran.r-project.org/).

2.5. TIME composition analysis

The immune score (IS) of the COAD samples were determined using the 'Estimate of STromal and Immune Cells in MAlignant Tumors using Expression data' (ESTIMATE) algorithm with transcriptome data (FPKM) [27]. Additionally, we obtained the gene set of pan-cancer metagenes for 28 immune cell types [28]. Subsequently, we inferred the proportions of 28 types of infiltrating immune cells based on the expression levels using the ssGSEA in R package "GSVA" (v1.50.0) (https://bioconductor.org/) [23].

2.6. Differentially expressed gene (DEG) analyses

DEGs were identified using the R package "DESeq2" (v1.42.0) (https://bioconductor.org/) [27] based on the following thresholds: $|\log2\text{Fold-change}| > 1$ and adjusted $P < 0.001$ between high- and low-FS COAD subgroups with in the TCGA database. The matrix of gene-level read counts was used in the analysis.

2.7. Functional enrichment analysis

Gene Ontology (GO) biological process enrichment analyses for the DEGs between the high- and low-FS subgroups within the TCGA database were conducted via the web tool "Metascape" (https://metascape.org/) [29]. Benjamini-Hochberg (BH)-adjusted $P < 0.05$ was regarded as statistically significant.

2.8. Gene co-expression analysis

Weighted gene co-expression network analysis (WGCNA) was performed to analyze the co-expressed gene modules based on the transcriptome data obtained from the TCGA database using the WGCNA (v1.72-5) (https://cran.r-project.org/) package and automatic network construction method [30]. In this analysis, we used the 'blockwiseModules' function for network construction and module detection in the expression matrix. This function initially pre-clusters nodes (genes) into large clusters, known as blocks, using a variant of k-means clustering. Subsequently, hierarchical clustering is applied to each block, and modules are defined as branches of the resulting dendrogram.

2.9. Real-time quantitative polymerase chain reaction (RT-qPCR)

To validate the expression of the genes (e.g., *RP11-284N8.3*, *RP11-291B21.2* and *RP11-399O19.9*) in the co-expression module of interest from the TCGA database, we used RT-qPCR to detect the expression levels in tumor tissues and adjacent normal colon tissues from colon cancer patients. Tissue samples of colon cancer were obtained from surgical specimens at Yunnan Cancer Hospital. Colon cancer tissues and adjacent normal tissues from twenty patients were collected. Total RNA was extracted from the tissues using TRIzol reagent (15596026, Invitrogen, USA) and then was reverse transcribed using the GoScriptTM reverse transcription system (A5001, Promega, USA) according to the manufacturer's protocols. RT-qPCR of the target genes was performed with gene-specific primers using the GoTaq qPCR Master Mix (A6002, Promega, USA). The comparative cycle threshold method was applied for quantification of gene expression, and values were normalized to β-actin (ACTB). The primers are listed in Supplementary Table 1.

2.10. Immunohistochemical staining

To confirm the findings of the gene expression analysis, we performed immunohistochemical assays on formalin-fixed paraffin-embedded (FFPE) anonymized lesion samples of colon cancer tissue from three patients, obtained from the Pathology Department of Yunnan Cancer Hospital. We stained for FLT3 (1:500; catalog no. ab263452, Abcam) and CD66B (1:20000; catalog no. ab300122,

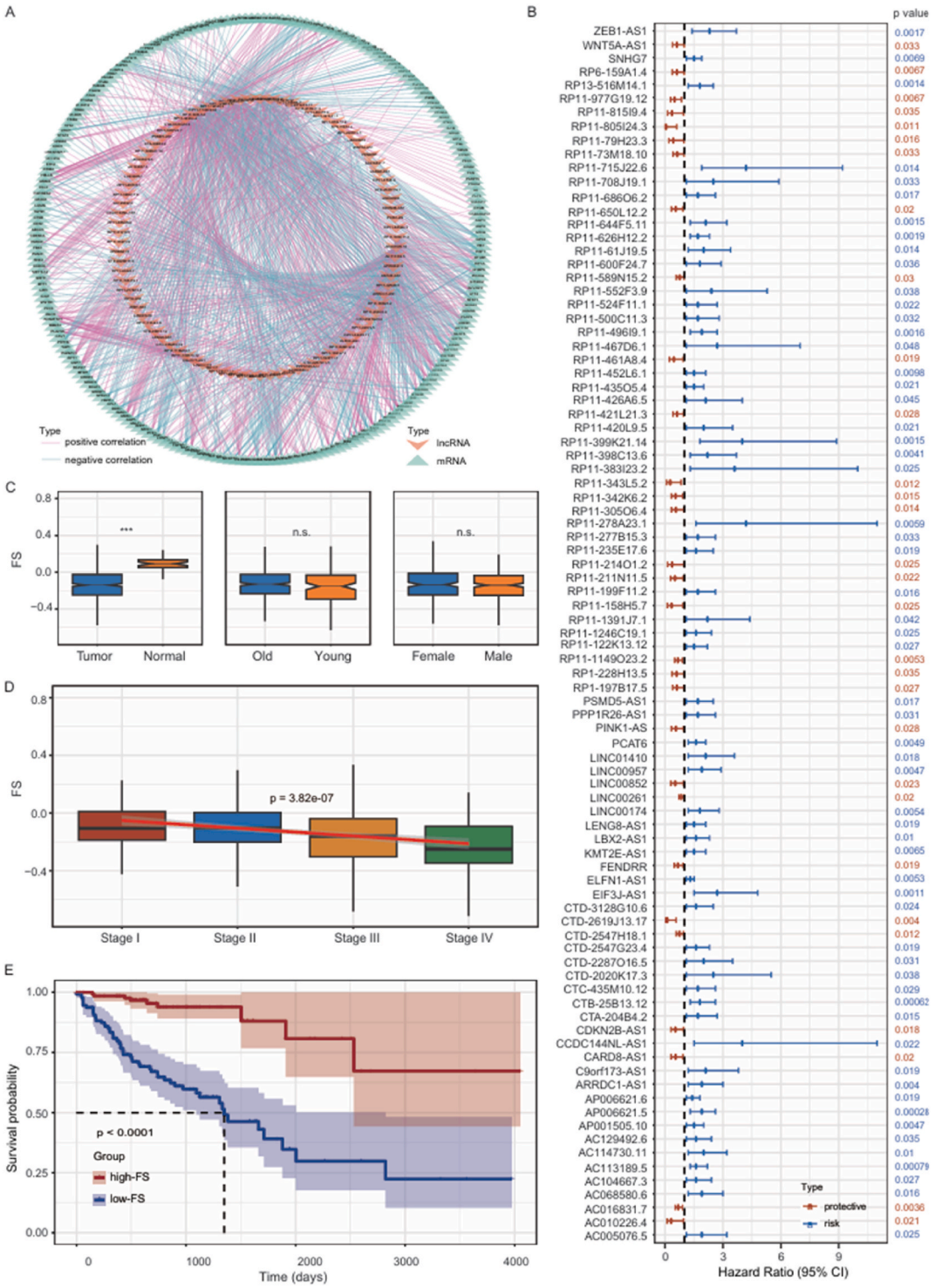

Fig. 1. Association between FS and COAD overall survival. (A) Co-expression relationships between ferr-lncRNAs (ferroptosis-related lncRNA genes) and ferr-mRNAs (ferroptosis-related mRNA genes). (B) Association between expression level of each ferr-lncRNA and COAD survival by univariate Cox model. (C) FS (ferroptosis score) differences in tumor and normal (paracancer) tissue samples, as well as tumor samples of different sex and age. (D) FS was decreased with pathological stage in COAD samples. (E) Kaplan-Meier survival curve of high- and low-FS subgroups. (***: $P < 0.001$; n.s.: non-significant; CI: Confidence Interval).

Abcam). Detailed steps: Deparaffinize the paraffin sections to water and perform antigen retrieval. After retrieval, let the sections cool naturally and wash them in PBS (pH 7.4) 3 times for 5 min each to block endogenous peroxidase. Next, place the sections in 3 % hydrogen peroxide solution, incubate at room temperature protected from light for 25 min, and then wash them in PBS 3 times for 5 min each. Add 3 % BSA to the tissue sections and incubate at room temperature for 30 min. After removing the blocking solution, add the primary antibody diluted in PBS to the sections and incubate overnight at 4 °C. Wash the sections in PBS 3 times for 5 min each, then add the HRP-labeled secondary antibody corresponding to the primary antibody and incubate at room temperature for 50 min. Wash the sections in PBS 3 times for 5 min each, then add freshly prepared DAB staining solution, controlling the staining time under a microscope. Terminate the staining by washing the sections with tap water. Counterstain with hematoxylin for about 3 min, wash with tap water, differentiate briefly, wash again, and return to blue under running water. Dehydrate the sections sequentially in 75 % alcohol for 5 min, 85 % alcohol for 5 min, anhydrous ethanol I for 5 min, anhydrous ethanol II for 5 min, and xylene I for 5 min. Allow the sections to air dry slightly and then mount them with mounting medium. Finally, examine and interpret the results under a bright-field microscope. The nucleus of hematoxylin in stain is blue, and the positive signal of DAB is brown-yellow.

2.11. Statistical analysis

R software (v4.3.1; https://cran.r-project.org/) was performed for statistical analyses. Pearson's correlation test was employed to assess the correlation between two features, and Student's *t*-test was used to evaluate difference in the features of interest between two groups.

3. Results

3.1. Clinical characteristics of COAD samples

Clinical information on the 446 COAD samples from TCGA was presented in Supplementary Table 2. Results showed that both age and pathological stage were associated with COAD prognosis, with a significance level of $P < 0.05$. However, there was no significant

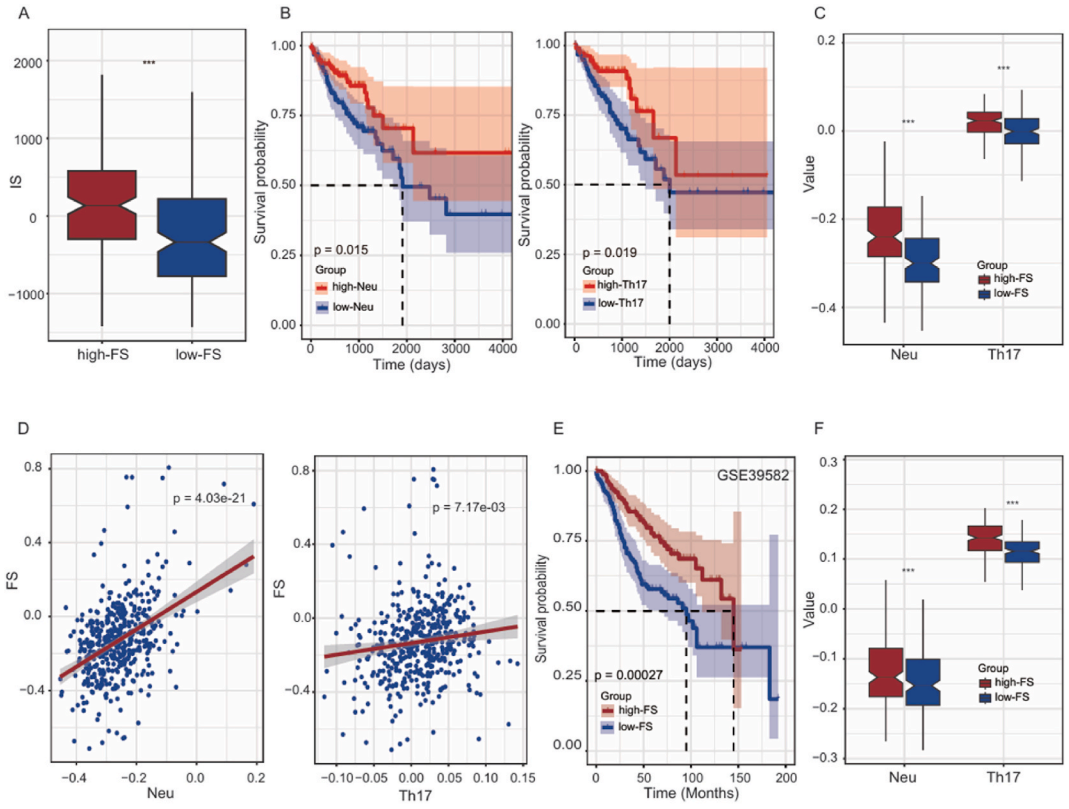

Fig. 2. Association between FS and TIME in COAD samples. (A) High-FS COAD subgroup displayed a high IS (immune score). (B) High infiltration levels of Neu (neutrophils) and Th17 (type 17 T helper cells) are associated to improved COAD survival ($P < 0.05$). (C) Infiltration differences of the two immune cells between the high- and low-FS COAD subgroups. (D) Correlations between the infiltration levels of two immune cells and FSs in COAD samples. (E) The high-FS COAD subgroup showed a good survival probability according to the GSE39582 dataset. (F) Increased infiltration levels of Neu and Th17 cells in high-FS COAD subgroup based on the GSE39582 dataset. (***: $P < 0.001$).

association between samples' sex and prognosis.

3.2. Classifying COAD samples by inferred ferroptosis activity

Initially, we identified 1778 ferr-lncRNAs that co-expressed with any of the 385 ferr-mRNAs retrieved from the FerrDb (V2) database, with the thresholds of P value < 0.00001 and absolute correlation coefficient >0.4. Subsequently, univariate Cox regression analyses pinpointed 30 positively and 59 negatively associated ferr-lncRNAs with COAD survival ($P < 0.05$) (Fig. 1A and B). FS index, representing ferroptosis activity, was then estimated based on the expression of the 89 ferr-lncRNAs using ssGSEA (see Materials and Methods). The results revealed FSs ranging from −0.71 to 0.81 (Supplementary Fig. 1), with tumor samples exhibiting decreased FS compared to normal samples (Fig. 1C). No significant differences in FSs were observed between the male and female samples (Fig. 1C), as well as between the young (age <60 years) and old (age >60 years) groups (Fig. 1C). Notably, we observed decreased FSs in samples at the late pathological stage, indicating an association between FS and tumor progression (Fig. 1D). Subsequently, we separated COAD samples into high- and low-FS subgroups (see Materials and Methods; high-FS subgroup refers to samples with FSs greater than the 75th percentile, while low-FS subgroup corresponds to samples with FSs lower than the 25th percentile). Kaplan-Meier survival analysis showed that high-FS subgroup exhibited a favorable survival outcome ($P < 0.0001$) (Fig. 1E), which was further validated by multivariate Cox regression analysis after correcting for age, sex, and pathological stage (Supplementary Fig. 2).

3.3. Interaction of ferroptosis and tumor immune microenvironment in COAD classification and progression

Currently, there is emerging evidence suggesting a connection between ferroptosis activity and TIME, influencing the progression and therapy of various cancers. To explore this association, we estimated the IS, serving as an index of immune cell infiltration in tumor microenvironment, for each sample using the ESTIMATE method. Results showed that high-FS COAD subgroup displayed elevated ISs (Fig. 2A), and FSs were positively correlated with ISs (Supplementary Fig. 3), indicating a significant association between ferroptosis and TIME in COAD development.

To further elucidate the infiltrating immune cells involved to the TIME differences in the FS based COAD subgroups, we inferred the infiltration levels (i.e., enrichment scores) of 28 immune cell types in the TIME of samples, based on the expression levels of 782 metagenes using ssGSEA package. Among these immune cell types, neutrophils (Neu) and type 17 T helper cells (Th17) both exhibited positive associations between their infiltration levels and COAD survival (Fig. 2B and Supplementary Table 3). Consistently, results demonstrated increased infiltration of these two immune cells in high-FS subgroup compared to that in low-FS subgroup (Fig. 2C). Furthermore, we calculated the associations between immune infiltration and FS, and found Neu and Th17 cells were significantly positively associated with FSs in COAD samples (Fig. 2D). Taken together, these findings indicate an interplay between tumor cell ferroptosis and Neu and Th17 cells in the TIME, contributing to COAD progression.

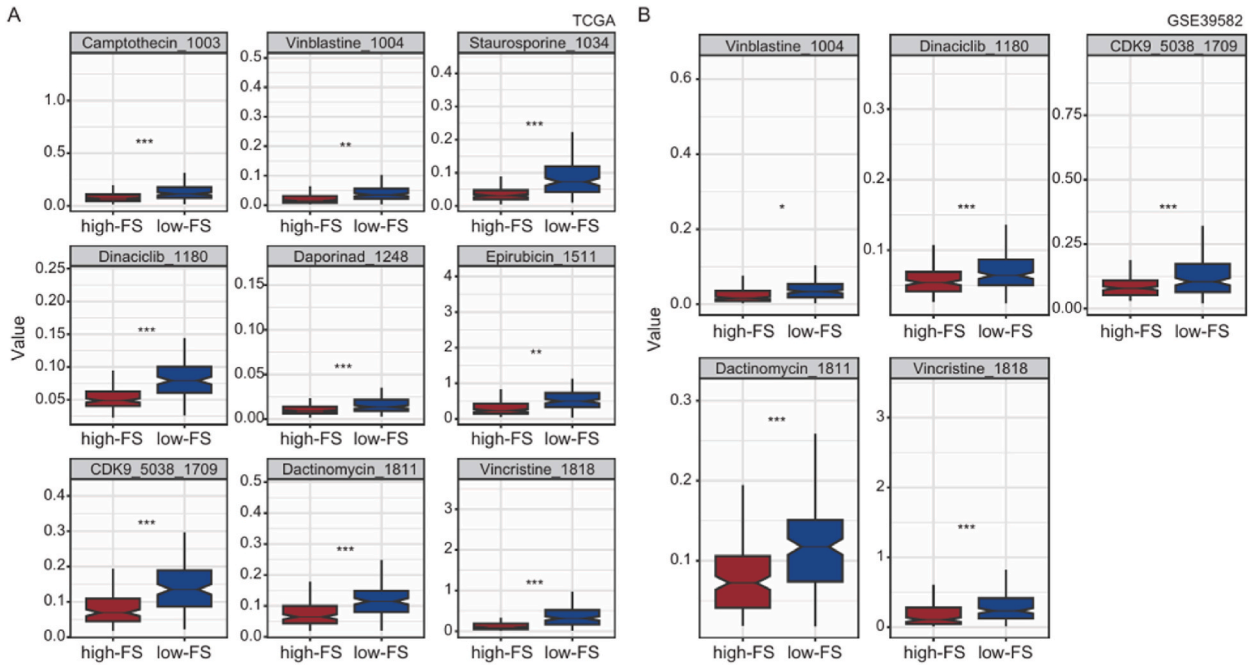

Fig. 3. Drug sensitivity between high- and low-FS COAD subgroups. (A) Differences in predicted drug sensitivity between high- and low-FS subgroups from the TCGA dataset. (B) Differences in predicted drug sensitivity between high- and low-FS subgroups from the GSE39582 dataset. (*: $P < 0.05$; **: $P < 0.01$; ***: $P < 0.001$; The y-axis value refers to the IC50 (half-maximal inhibitory concentration)).

To test whether the findings can be observed in other COAD samples, we collected and analyzed another gene expression dataset containing 566 tumor samples (GSE39582). Similarly, ssGSEA method was used to infer the FS of each COAD sample based on the expression of the previously identified ferr-lncRNAs. Consistently, results showed that the samples with high FS exhibited a favorable survival probability (Fig. 2E). Furthermore, increased infiltration levels of Neu and Th17 cells were also observed in the high-FS subgroup (Fig. 2F). These findings indicate that the association between high FS, improved survival, and enhanced infiltration of certain immune cells (i.e., Neu and Th17) is consistent across different COAD samples.

3.4. A high drug sensitivity in COAD samples with high FS

To explore the potential association between FS and COAD treatment precision, we estimated the drug sensitivity score of each sample using the R package "oncoPredict", based on drug sensitivity data from the GDSC database. We identified nine agents that showed sensitivity differences between the high- and low-FS COAD subgroups, with high drug sensitivity observed in the high-FS subgroup from TCGA dataset (Fig. 3A). Additionally, five of these nine agents also displayed high sensitivity in the high-FS subgroup from the GSE39582 dataset (Fig. 3B). Among these drugs, several (e.g., vinblastine, dinaciclib) have been used in COAD therapy [31,32], likely indicating a potential of the FS-based COAD classification in guiding precision medication.

3.5. Identification of lncRNA-mRNA co-expression networks involved to ferroptosis, immune infiltration and COAD progression

Subsequently, we analyzed changes in gene expression within the TCGA database, identifying 2332 DEGs between high- and low-FS subgroups, including 1447 up-regulated and 885 down-regulated genes (Fig. 4A; see Materials and Methods). To investigate the variations in biological functions and signaling pathways between the two subgroups, we performed functional enrichment analysis on the DEGs. The findings revealed that the up-regulated genes were enriched in pathways including the inflammatory response, positive regulation of cytokine production, cytokine-mediated signaling pathway, regulation of immune effector process, etc. (Fig. 4B). The down-regulated genes were enriched in pathways involved in inorganic ion transmembrane transport, organic hydroxy compound transport, response to metal ion, etc. (Supplementary Fig. 4).

Recognizing that the 1447 up-regulated genes in high-FS subgroup have a greater potential for linking ferroptosis and TIME implicated in COAD suppression, we focused on their expression and used WGCNA to construct the lncRNA-mRNA co-expression networks. In total, we obtained two co-expression modules (see Materials and Methods), displayed in different colors, including orange

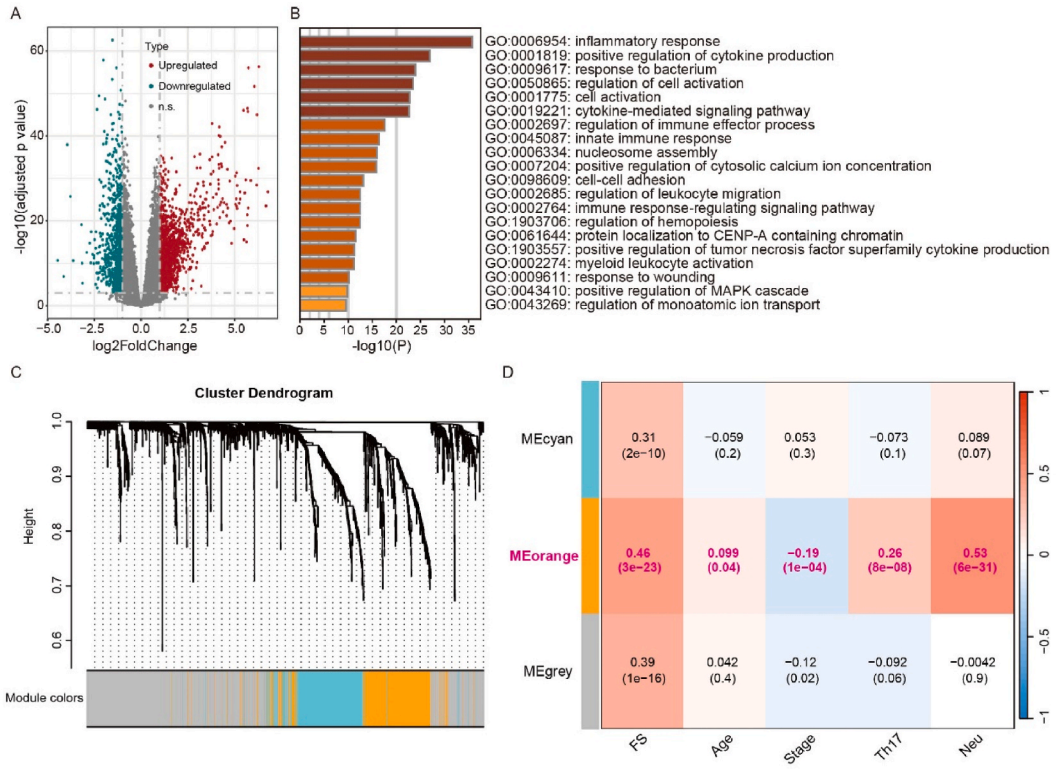

Fig. 4. Co-expression gene modules for DE-lncRNAs and DE-mRNAs between high- and low-FS COAD subgroups. (A) Volcano plot for the DEGs between the two subgroups. (B) GO biological enrichment analysis for the up-regulated genes in high-FS subgroup. (C) Cluster dendrogram of co-expressed gene modules. (D) Heatmap plot displaying correlation coefficients and *P* values for each module and clinical trait.

and cyan, as shown in Fig. 4C. These modules included 336 and 304 genes, respectively. To identify key modules associated with both tumor cell ferroptosis and TIME, we performed correlation analysis between the gene modules and clinical traits of interest. We found that the orange gene module was positively associated with the FSs and infiltration levels of Neu and Th17, while also negatively correlated with the COAD pathological stage (Fig. 4D). These findings highlight the potential roles of this gene module in the interplay between tumor cell ferroptosis and corresponding immune processes in COAD progression. The orange module comprises 39 lncRNAs and 297 mRNAs, including six identified as driver genes (viz., *HIF1A*, *FLT3*, *CYBB*, *IL1B*, *IFNG* and *IDO1*) of ferroptosis by retrieving the FerrDb (V2) database [22]. To validate the expression status of the genes in this module from TCGA database, we detected the expression levels of randomly selected 3 lncRNA genes (*RP11-284N8.3*, *RP11-291B21.2* and *RP11-399O19.9*) in tumor tissues and adjacent normal colon tissues from twenty patients with colon cancer using RT-qPCR method. Results showed that the genes were all downregulated in tumor tissues (Fig. 5A), consistent with the expression trends observed in TCGA data (Fig. 5B). Moreover, we selected *FLT3* [33], *MMP25* [34], and *RORC* [35] as marker genes for tumor cell ferroptosis, Neu infiltration, and Th17 infiltration, respectively, and detected their expression differences between colon tumor tissues and adjacent normal colon tissues. RT-qPCR results demonstrated the downregulation of all three genes in colon tumor tissues, suggesting positive associations between tumor ferroptosis and infiltration levels of Neu and Th17 cells (Fig. 5A), which also align with the results from TCGA data (Fig. 5B). Additionally, immunohistochemical staining of FLT3 [33] and CD66B [36] in colon cancer tissues further supported the positive association between tumor cell ferroptosis and Neu infiltration (Supplementary Fig. 5). Further biological process analysis showed that the genes in this module were enriched in immune-related biological process, such as inflammatory response, innate immune response, immune response-regulating signaling pathway, regulation of immune effector response, etc. (Fig. 6A and B).

Moreover, to identify key ferr-lncRNAs with potential implications for COAD diagnosis, we input the 39 lncRNAs obtained from the orange module in a LASSO Cox regression model. This analysis identified four ferr-lncRNAs (viz., *RP11-1008C21.1*, *RP11-399O19.9*, *RP11-576I22.2*, *RP6-159A1.4*; Fig. 6C), among which *RP11-399O19.9* was also detected in the GSE39582 dataset and was upregulated in the high-FS subgroup (Fig. 6C). Based on the gene expression level and coefficient value of each ferr-lncRNA, we evaluated the risk score for each sample using the model: risk score = (−0.4042***RP11-1008C21.1*) + (−1.3001***RP11-399O19.9*) + (−1.2507***RP11-576I22.2*) + (−0.7126***RP6-159A1.4*). Kaplan-Meier survival analysis showed that COAD samples with high-risk scores had poorer survival probability (Fig. 6D). Fig. 6D also displayed receiver operating characteristic (ROC) curves for COAD samples at 1-, 3- and 5-year, with area under the curves (AUCs) equaling to 0.757, 0.711 and 0.683, respectively. Collectively, these findings indicate that the lncRNA-mRNA co-expression network may play an important role in COAD suppression via linking the increased ferroptosis of tumor cells and Neu and Th17 cell infiltration in the tumor microenvironment.

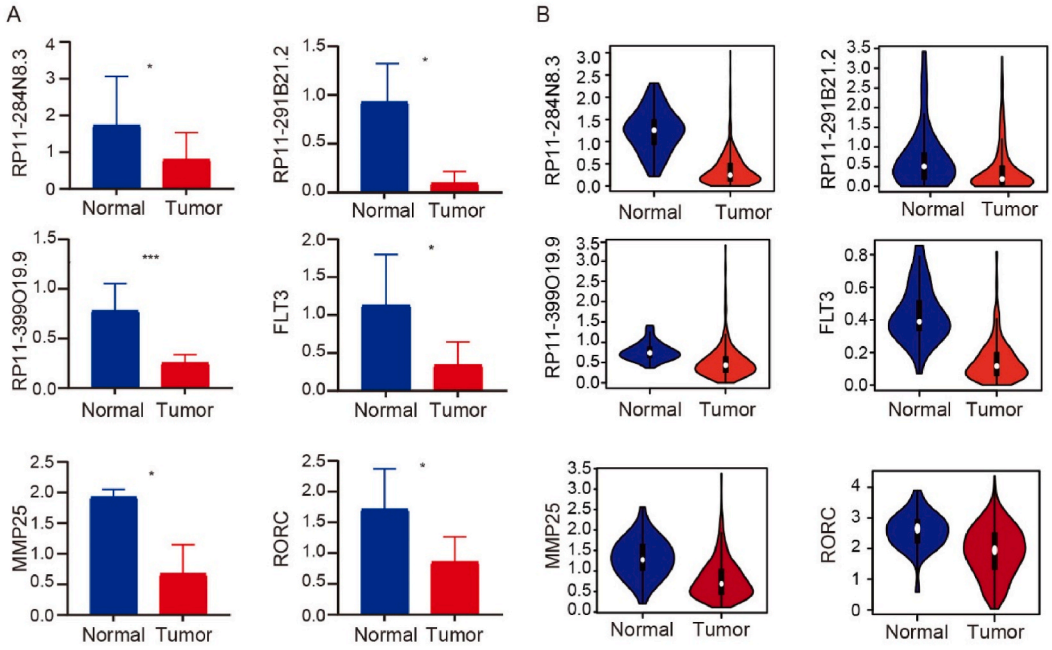

Fig. 5. RT-qPCR validation of expression differences of six genes between colon cancer tissues and adjacent normal tissues in colon patients. (A) RT-qPCR result showing the downregulation of the three lncRNA genes (viz., *RP11-284N8.3*, *RP11-291B21.2*, and *RP11-399O19.9*) and the three protein-coding genes (viz., *FLT3*, *MMP25*, and *RORC*) in tumor tissues compared to adjacent normal colon tissues from COAD patients. (B) The three lncRNA genes and three protein-coding genes presenting reduced expression in tumor tissues corresponding to normal tissues of COAD samples based on the TCGA data. (*: $P < 0.05$; ***: $P < 0.001$; The y-axis value refers to the value of gene expression).

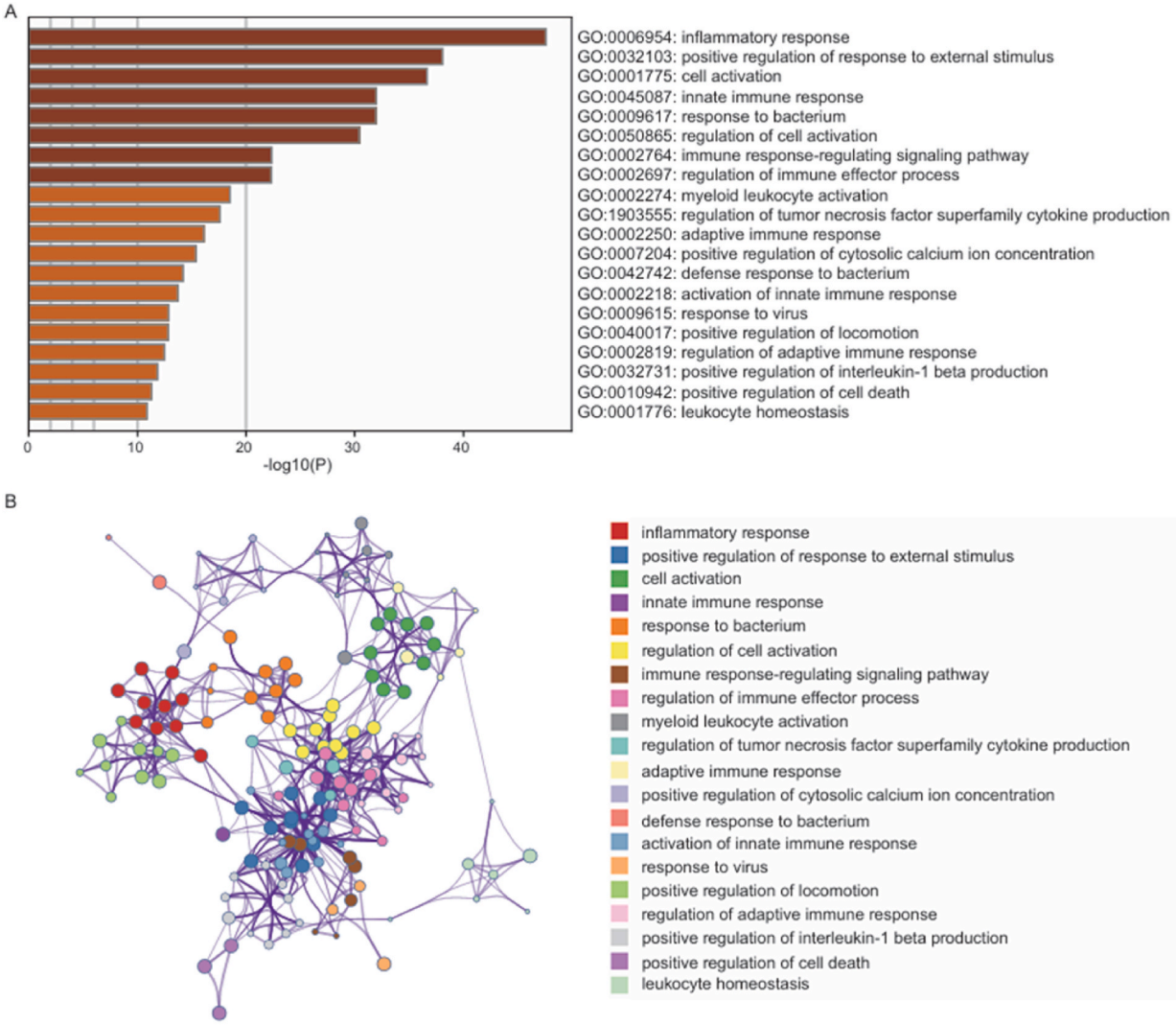

(caption on next page)

Fig. 6. Potential association between orange module and COAD suppression. (A–B) Biological process enrichment analysis for the genes in the orange module. (C) Expression differences of several ferr-lncRNAs in high- and low-FS subgroups from TCGA and GSE39582 datasets. (D) Survival curves for the COAD samples with high- and low-risk scores, and ROC (receiver operating characteristic) curves and corresponding AUC (area under the curve) values for the 1-, 3- and 5-year overall survival in the COAD samples.

4. Discussion

Ferroptosis is a new type of iron-dependent programmed cell death, characterized by intracellular accumulation of detrimental lipid reactive oxygen species (ROS) [37]. There is accumulating evidence suggesting that abnormal alterations in ferroptosis activity are closely associated with the pathogenesis of various diseases, especially tumors [38]. Moreover, the activation or blockade of the iron metabolism pathway has proven to be an effective strategy for mitigating the progression of multiple cancers, including COAD [39]. Currently, a growing body of evidence indicates that tumor cell ferroptosis is closely associated with the TIME, which plays important roles in influencing tumor initiation and metastasis and therapy [40]. Therefore, understanding the underlying regulatory mechanisms bridging ferroptosis and TIME offers a new perspective on anticancer therapy and has the potential to be leveraged for COAD diagnosis and classification.

In this study, we employed FSs to assess the ferroptosis activity of each COAD sample, based on the expression of 89 lncRNAs associated with ferr-mRNAs and COAD survival, using ssGSEA. Our results demonstrated a negative association between FSs and COAD pathological stage, as well as a positive association with COAD survival, suggesting a close correlation between inferred FS and COAD progression. In addition, a recent systematic review and meta-analysis demonstrated that promoting ferroptosis significantly benefits cancer prognosis [41]. Moreover, we observed a positive correlation between FS and IS in the COAD samples, a similar trend was also observed in other cancer types, such as gastric cancer [42]. Since the correlation between various immune cells in the TIME and ferroptosis of colon cancer cells is not well understood, we estimated the infiltration levels of immune cells in the tumor microenvironment of each sample. Notably, we observed an association between ferroptosis activity and the TIME in COAD samples, with high-FS subgroup (i.e., samples with FSs above the 75th percentile) displaying an increase in Neu and Th17 cell infiltration compared to low-FS subgroup (i.e., samples with FSs below the 25th percentile). The role of Neu in cancer is complex, with studies suggesting both tumor-suppressive and tumor promoting functions [43–45]. Our analysis showed that the inferred level of Neu infiltration is positively associated to COAD survival, aligning with previous studies suggesting that high infiltration of Neu is a favorable prognostic factor in colorectal cancer and gastric cancer [46–48]. Moreover, evidence suggests that Neu can secrete myeloperoxidase-containing granules, which have the potential to induce ferroptosis and kill tumor cells [49]. Similarly, studies have implicated Th17 cells in the TIME, highlighting their role in antitumor immunity [50–52]. Taken together, these findings indicate a potential scenario in which increased Neu and Th17 cell infiltration in the TIME could induce tumor cell ferroptosis, thereby suppressing COAD progression. Nonetheless, growing evidence supports the high heterogeneity among Neu within the TIME, where they exhibit both pro-tumor and anti-tumor roles [53,54], underscoring the need for further investigation into the relationship between Neu subtypes and tumor ferroptosis.

In addition, we observed that the high-FS COAD subgroup exhibited a tendency towards increased sensitivity to several anti-cancer drugs, such as vinblastine and dinaciclib. Similar reports indicating the association between elevated ferroptosis activity and increased drug sensitivity have also been documented in some other cancer types, such as breast cancer and gastric cancer [55,56]. Although direct studies linking ferroptosis with these drugs are relative limited at present, the principle that ferroptosis inducers can enhance the efficacy of chemotherapy drugs is gradually established. For example, a study showed that supplementing with RSL3, a ferroptosis activator, can potentiate the effects of chemotherapeutic agent 5-fluorouracil against colorectal cancer cells [57]. These findings reinforce the potential of inducing ferroptosis to overcome chemotherapy resistance in cancer and emphasize the clinical significance of using ferroptosis inducers in conjunction with chemotherapy drugs to enhance the effectiveness of COAD treatment and improve patient outcomes.

To explore the biological processes associated with tumor cell ferroptosis and TIME in COAD samples, we performed differential gene expression analysis and functional enrichment analysis. Our results revealed that the up-regulated genes in high-FS subgroup were enriched in the immune-related biological processes (e.g., inflammatory response, positive regulation of cytokine production, regulation of immune effector process). Notably, several of these processes have been implicated in ferroptosis and cancer development. For example, chemokines, closely related to inflammation, can affect both ferroptosis and tumor progression [58]. These findings suggest an interaction between ferroptosis and the TIME interact in the pathological development of COAD. Furthermore, we identified a lncRNA-mRNA co-expression network (i.e., orange module) that was upregulated in high-FS subgroup and displayed close associations with both the FS and the Neu and Th17 cell infiltration in COAD samples. Many genes in this module are associated with tumor pathogenesis, including the ferroptosis-driving gene *FLT3*, implicated in growth-suppressive functions in various human cancer cells [59]. Additionally, the decreased expression level of *RP11-399O19.9* in tumor tissues corresponding to normal tissues in the TCGA dataset was validated by RT-qPCR result in another COAD cohort from Cheng's study [60]. In summary, these findings support the potential roles of the lncRNA-mRNA co-expression network in COAD suppression by linking ferroptosis process and immune infiltration in the tumor microenvironment.

5. Conclusion

In summary, we estimated the ferroptosis activity and immune cell infiltration of COAD samples based on the transcriptome data,

and provided new evidence supporting that an increase in Neu and Th17 infiltration could improve COAD survival through provoking the ferroptosis activity of colon cancer cells. In addition, we identified a key lncRNA-mRNA network that were correlated with the interplay of tumor cell ferroptosis and Neu and Th17 cell infiltration implicated in COAD progression. Further clinical and experimental assays would aid in elucidating the roles of identified lncRNAs in linking ferroptosis and immune response, and thereby contributing to our understanding of COAD development and therapy.

Ethics approval

This study was performed in line with the principles of the Declaration of Helsinki and approved by the Ethics Committee of the Third Affiliated Hospital, Kunming Medical University, China (KYCS2024-027).

Funding

This work was supported by grants from Joint Special Fund Project of Yunnan Provincial Science and Technology Department-Kunming Medical University (202401AY070001-328), China; the Scientific Research Fund Project of Yunnan Provincial Department of Education (2023Y0657), China; Yunnan Fundamental Research Project (202201AS070080, 202401AW070011), China; Joint Special Fund Project of Yunnan Provincial Science and Technology Department-Kunming Medical University (202201AY070001-134), China; the Reserve Talent Project of Young and Middle-aged Academic and Technical Leaders in Yunnan Province (202305AC160029), China; National Natural Science Foundation of China (82060516), China.

Data availability statement

The initial high-throughput datasets are available in The Cancer Genome Atlas (TCGA) and Gene Expression Omnibus (GEO) databases.

CRediT authorship contribution statement

Xiao-Qiong Chen: Writing – review & editing, Writing – original draft, Methodology, Investigation, Funding acquisition, Formal analysis, Data curation. **Xuan Zhang:** Writing – review & editing, Validation. **Ding-Guo Pan:** Writing – review & editing, Methodology. **Guo-Yu Li:** Investigation. **Rui-Xi Hu:** Data curation. **Tao Wu:** Formal analysis. **Tao Shen:** Methodology. **Xin-Yi Cai:** Validation. **Xian-Shuo Cheng:** Writing – review & editing. **Junying Qin:** Writing – review & editing. **Fu-Hui Xiao:** Writing – review & editing, Project administration, Funding acquisition. **Yun-Feng Li:** Writing – review & editing, Validation, Supervision, Project administration, Funding acquisition.

Declaration of competing interest

The authors declare that they have no known competing financial interests or personal relationships that could have appeared to influence the work reported in this paper.

Acknowledgements

Not applicable.

Abbreviations

COAD	colon adenocarcinoma
TCGA	the Cancer Genome Atlas
FS	ferroptosis score
ssGSEA	single-sample gene set enrichment analysis
DEG	differentially expressed gene
Neu	neutrophils
Th17	type 17 T helper cell
TIME	tumor immune microenvironment

Appendix A. Supplementary data

Supplementary data to this article can be found online at https://doi.org/10.1016/j.heliyon.2024.e33738.

References

[1] H. Sung, J. Ferlay, R.L. Siegel, M. Laversanne, I. Soerjomataram, A. Jemal, et al., Global cancer statistics 2020: GLOBOCAN estimates of incidence and mortality worldwide for 36 cancers in 185 countries, Ca-Cancer J. Clin. 71 (3) (2021) 209–249.
[2] W. Chen, R. Zheng, P.D. Baade, S. Zhang, H. Zeng, F. Bray, et al., Cancer statistics in China, 2015, Ca-Cancer J. Clin. 66 (2016) 115–132.
[3] L. Ye, T. Zhang, Z. Kang, G. Guo, Y. Sun, K. Lin, et al., Tumor-infiltrating immune cells act as a marker for prognosis in colorectal cancer, Front. Immunol. 10 (2019) 2368.
[4] A. Janney, F. Powrie, E.H. Mann, Host–microbiota maladaptation in colorectal cancer, Nature 585 (2020) 509–517.
[5] A. Valdeolivas, B. Amberg, N. Giroud, M. Richardson, E.J.C. Gálvez, S. Badillo, et al., Profiling the heterogeneity of colorectal cancer consensus molecular subtypes using spatial transcriptomics, Npj Precis Onc 8 (2024) 1–16.
[6] Y. Xie, W. Hou, X. Song, Y. Yu, J. Huang, X. Sun, et al., Ferroptosis: process and function, Cell Death Differ. 23 (2016) 369–379.
[7] J. Liang, D. Wang, H. Lin, X. Chen, H. Yang, Y. Zheng, et al., A novel ferroptosis-related gene signature for overall survival prediction in patients with hepatocellular carcinoma, Int. J. Biol. Sci. 16 (2020) 2430–2441.
[8] L. Li, C. Qiu, M. Hou, X. Wang, C. Huang, J. Zou, et al., Ferroptosis in ovarian cancer: a novel therapeutic strategy, Front. Oncol. 11 (2021) 665945.
[9] Y. Wang, H. Xia, Z. Chen, L. Meng, A. Xu, Identification of a ferroptosis-related gene signature predictive model in colon cancer, World J. Surg. Oncol. 19 (2021) 135.
[10] Z.H. Wu, Y. Tang, H. Yu, H.D. Li, The role of ferroptosis in breast cancer patients: a comprehensive analysis, Cell Death Dis. 7 (2021) 93.
[11] W. Wang, M. Green, J.E. Choi, M. Gijón, P.D. Kennedy, J.K. Johnson, et al., CD8+ T cells regulate tumour ferroptosis during cancer immunotherapy, Nature 569 (2019) 270–274.
[12] I. Efimova, E. Catanzaro, L.V. der Meeren, V.D. Turubanova, H. Hammad, T.A. Mishchenko, et al., Vaccination with early ferroptotic cancer cells induces efficient antitumor immunity, J Immunother Cancer 8 (2020) e001369.
[13] H. Xu, D. Ye, M. Ren, H. Zhang, F. Bi, Ferroptosis in the tumor microenvironment: perspectives for immunotherapy, Trends Mol. Med. 27 (2021) 856–867.
[14] B. Wiernicki, S. Maschalidi, J. Pinney, S. Adjemian, T. Vanden Berghe, K.S. Ravichandran, et al., Cancer cells dying from ferroptosis impede dendritic cell-mediated anti-tumor immunity, Nat. Commun. 13 (2022) 3676.
[15] L. Statello, C.J. Guo, L.L. Chen, M. Huarte, Gene regulation by long non-coding RNAs and its biological functions, Nat. Rev. Mol. Cell Biol. 22 (2021) 96–118.
[16] B. Xie, Y. Guo, Molecular mechanism of cell ferroptosis and research progress in regulation of ferroptosis by noncoding RNAs in tumor cells, Cell Death Dis. 7 (2021) 101.
[17] D. Huang, J. Chen, L. Yang, Q. Ouyang, J. Li, L. Lao, et al., NKILA lncRNA promotes tumor immune evasion by sensitizing T cells to activation-induced cell death, Nat. Immunol. 19 (2018) 1112–1125.
[18] E.G. Park, S.J. Pyo, Y. Cui, S.H. Yoon, J.W. Nam, Tumor immune microenvironment lncRNAs, Briefings Bioinf. 23 (2022) bbab504.
[19] M.J. Goldman, B. Craft, M. Hastie, K. Repečka, F. McDade, A. Kamath, et al., Visualizing and interpreting cancer genomics data via the Xena platform, Nat. Biotechnol. 38 (2020) 675–678.
[20] L. Marisa, A. de Reyniès, A. Duval, J. Selves, M.P. Gaub, L. Vescovo, et al., Gene expression classification of colon cancer into molecular subtypes: characterization, validation, and prognostic value, PLoS Med. 10 (2013) e1001453.
[21] B.M. Bolstad, R.A. Irizarry, M. Åstrand, T.P. Speed, A comparison of normalization methods for high densityoligonucleotide array data based on variance and bias, Bioinformatics 19 (2003) 185–193.
[22] N. Zhou, X. Yuan, Q. Du, Z. Zhang, X. Shi, J. Bao, et al., FerrDb V2: update of the manually curated database of ferroptosis regulators and ferroptosis-disease associations, Nucleic Acids Res. 51 (2023) D571–D582.
[23] S. Hänzelmann, R. Castelo, J. Guinney, GSVA: gene set variation analysis for microarray and RNA-Seq data, BMC Bioinf. 14 (2013) 7.
[24] W. Yang, J. Soares, P. Greninger, E.J. Edelman, H. Lightfoot, S. Forbes, et al., Genomics of Drug Sensitivity in Cancer (GDSC): a resource for therapeutic biomarker discovery in cancer cells, Nucleic Acids Res. 41 (2012) D955–D961.
[25] F. Iorio, T.A. Knijnenburg, D.J. Vis, G.R. Bignell, M.P. Menden, M. Schubert, et al., A landscape of pharmacogenomic interactions in cancer, Cell 166 (2016) 740–754.
[26] D. Maeser, R.F. Gruener, R.S. Huang, oncoPredict: an R package for predicting in vivo or cancer patient drug response and biomarkers from cell line screening data, Briefings Bioinf. 22 (2021) bbab260.
[27] M.I. Love, W. Huber, S. Anders, Moderated estimation of fold change and dispersion for RNA-seq data with DESeq2, Genome Biol. 15 (2014) 550.
[28] P. Charoentong, F. Finotello, M. Angelova, C. Mayer, M. Efremova, D. Rieder, et al., Pan-cancer immunogenomic analyses reveal genotype-immunophenotype relationships and predictors of response to checkpoint blockade, Cell Rep. 18 (2017) 248–262.
[29] Y. Zhou, B. Zhou, L. Pache, M. Chang, A.H. Khodabakhshi, O. Tanaseichuk, et al., Metascape provides a biologist-oriented resource for the analysis of systems-level datasets, Nat. Commun. 10 (2019) 1523.
[30] P. Langfelder, S. Horvath, WGCNA: an R package for weighted correlation network analysis, BMC Bioinf. 9 (2008) 559.
[31] K.K.W. Auyeung, P.C. Law, J.K.S. Ko, Combined therapeutic effects of vinblastine and Astragalus saponins in human colon cancer cells and tumor xenograft via inhibition of tumor growth and proangiogenic factors, Nutr. Cancer 66 (2014) 662–674.
[32] M. Zhang, L. Zhang, R. Hei, X. Li, H. Cai, X. Wu, et al., CDK inhibitors in cancer therapy, an overview of recent development, Am. J. Cancer Res. 11 (2021) 1913–1935.
[33] Y. Zheng, Y. Su, L. Ruan, Q. He, L. Gong, J. Li, Screening and biomarker assessment of ferroptosis genes *FLT3* and *ALOX5* in lung adenocarcinoma, Oncologie 25 (2023) 281–289.
[34] A.E. Starr, C.L. Bellac, A. Dufour, V. Goebeler, C.M. Overall, Biochemical characterization and N-terminomics analysis of leukolysin, the membrane-type 6 matrix metalloprotease (MMP25), J. Biol. Chem. 287 (2012) 13382–13395.
[35] C. Guntermann, A. Piaia, M.L. Hamel, D. Theil, T. Rubic-Schneider, A. Del Rio-Espinola, et al., Retinoic-acid-orphan-receptor-C inhibition suppresses Th17 cells and induces thymic aberrations, JCI Insight 2 (2017) e91127.
[36] J. Kargl, S.E. Busch, G.H.Y. Yang, K.H. Kim, M.L. Hanke, H.E. Metz, et al., Neutrophils dominate the immune cell composition in non-small cell lung cancer, Nat. Commun. 8 (2017) 14381.
[37] S.J. Dixon, J.A. Olzmann, The cell biology of ferroptosis, Nat. Rev. Mol. Cell Biol. 25 (2024) 1–19.
[38] G. Lei, L. Zhuang, B. Gan, Targeting ferroptosis as a vulnerability in cancer, Nat. Rev. Cancer 22 (2022) 381–396.
[39] J. Li, F. Cao, H. Yin, Z. Huang, Z. Lin, N. Mao, et al., Ferroptosis: past, present and future, Cell Death Dis. 11 (2020) 88.
[40] M. Binnewies, E.W. Roberts, K. Kersten, V. Chan, D.F. Fearon, M. Merad, et al., Understanding the tumor immune microenvironment (TIME) for effective therapy, Nat. Med. 24 (2018) 541–550.
[41] S. Li, K. Tao, H. Yun, J. Yang, Y. Meng, F. Zhang, et al., Ferroptosis is a protective factor for the prognosis of cancer patients: a systematic review and meta-analysis, BMC Cancer 24 (2024) 604.
[42] X. Jiang, F. Liu, P. Liu, Y. Yan, S. Lan, K. Zhuang, et al., Ferroptosis patterns correlate with immune microenvironment characterization in gastric cancer, Int. J. Gen. Med. 14 (2021) 6573–6586.
[43] A. Rakic, P. Beaudry, D.J. Mahoney, The complex interplay between neutrophils and cancer, Cell Tissue Res. 371 (2018) 517–529.
[44] M.E. Shaul, Z.G. Fridlender, The dual role of neutrophils in cancer, Semin. Immunol. 57 (2021) 101582.
[45] D. Wang, X. Li, D. Jiao, Y. Cai, L. Qian, Y. Shen, et al., LCN2 secreted by tissue-infiltrating neutrophils induces the ferroptosis and wasting of adipose and muscle tissues in lung cancer cachexia, J. Hematol. Oncol. 16 (2023) 30.
[46] M.L. Wikberg, A. Ling, X. Li, Å. Öberg, S. Edin, R. Palmqvist, Neutrophil infiltration is a favorable prognostic factor in early stages of colon cancer, Hum. Pathol. 68 (2017) 193–202.

[47] G. Sconocchia, I. Zlobec, A. Lugli, D. Calabrese, G. Iezzi, E. Karamitopoulou, et al., Tumor infiltration by FcγRIII (CD16)+ myeloid cells is associated with improved survival in patients with colorectal carcinoma, Int. J. Cancer 128 (2011) 2663–2672.
[48] R.A. Caruso, R. Bellocco, M. Pagano, G. Bertoli, L. Rigoli, C. Inferrera, Prognostic value of intratumoral neutrophils in advanced gastric carcinoma in a high-risk area in northern Italy, Mod. Pathol. 15 (2002) 831–837.
[49] P.P. Yee, Y. Wei, S.Y. Kim, T. Lu, S.Y. Chih, C. Lawson, et al., Neutrophil-induced ferroptosis promotes tumor necrosis in glioblastoma progression, Nat. Commun. 11 (2020) 5424.
[50] S. Nuñez, J.J. Saez, D. Fernandez, F. Flores-Santibañez, K. Alvarez, G. Tejon, et al., T helper type 17 cells contribute to anti-tumour immunity and promote the recruitment of T helper type 1 cells to the tumour, Immunology 139 (2013) 61–71.
[51] A. Schnell, D.R. Littman, V.K. Kuchroo, TH17 cell heterogeneity and its role in tissue inflammation, Nat. Immunol. 24 (2023) 19–29.
[52] W. Zou, N.P. Restifo, TH17 cells in tumour immunity and immunotherapy, Nat. Rev. Immunol. 10 (2010) 248–256.
[53] Y. Wu, J. Ma, X. Yang, F. Nan, T. Zhang, S. Ji, et al., Neutrophil profiling illuminates anti-tumor antigen-presenting potency, Cell 187 (2024) 1422–1439.e24.
[54] R. Xue, Q. Zhang, Q. Cao, R. Kong, X. Xiang, H. Liu, et al., Liver tumour immune microenvironment subtypes and neutrophil heterogeneity, Nature 612 (2022) 141–147.
[55] R. Sha, Y. Xu, C. Yuan, X. Sheng, Z. Wu, J. Peng, et al., Predictive and prognostic impact of ferroptosis-related genes ACSL4 and GPX4 on breast cancer treated with neoadjuvant chemotherapy, EBioMedicine 71 (2021) 103560.
[56] L. Shao, L. Zhu, R. Su, C. Yang, X. Gao, Y. Xu, et al., Baicalin enhances the chemotherapy sensitivity of oxaliplatin-resistant gastric cancer cells by activating p53-mediated ferroptosis, Sci. Rep. 14 (2024) 10745.
[57] X. Liu, S. Peng, G. Tang, G. Xu, Y. Xie, D. Shen, et al., Fasting-mimicking diet synergizes with ferroptosis against quiescent, chemotherapy-resistant cells, EBioMedicine 90 (2023) 104496.
[58] A.J. Ozga, M.T. Chow, A.D. Luster, Chemokines and the immune response to cancer, Immunity 54 (2021) 859–874.
[59] E. Oveland, L. Wergeland, R. Hovland, J.B. Lorens, B.T. Gjertsen, K.E. Fladmark, Ectopic expression of Flt3 kinase inhibits proliferation and promotes cell death in different human cancer cell lines, Cell Biol. Toxicol. 28 (2012) 201–212.
[60] Y. Cheng, L. Geng, K. Wang, J. Sun, W. Xu, S. Gong, et al., Long noncoding RNA expression signatures of colon cancer based on the ceRNA network and their prognostic value, Dis. Markers 2019 (2019) 1–13.